

Design of cryogenic system for the Beijing Electron Positron Collider II upgrade

Ruixiong Han^{a,b,c,*} Jiehao Zhang^{a,b} Liangrui Sun^{a,b} Miaofu Xu^{a,b} Xiaochen Yang^{a,b}
Minjing Sang^{a,b} Rui Ye^{a,b} Xiangzhen Zhang^{a,b,c} Penghui Li^{a,b,c} Zhuo Zhang^{a,b}
Tongxian Zhao^{a,b,c} Zhengze Chang^{a,b,c} Changcheng Ma^{a,b,c} Mei Li^{a,b}
Yongcheng Jiang^{a,b,c} Keyu Zhu^{a,b} Hao Chen^a Xin Liu^a Lu Zhang^a Libo Chang^a
Yang Guo^a Shaopeng Li^{a,b,c} and Rui Ge^{a,b,c}

^aAccelerator Division, Institute of High Energy Physics (IHEP), Chinese Academy of Sciences (CAS),
19B Yuquan Road, Beijing, 100049, Beijing, China

^bCenter for Superconducting RF and Cryogenics, Institute of High Energy Physics,
Chinese Academy of Sciences,
19B Yuquan Road, Beijing, 100049, Beijing 100049, China

^cSchool of Nuclear Science and Technology, University of Chinese Academy of Sciences,
19A Yuquan Road, Beijing, 100049, Beijing 100049, China

E-mail: hanrx@ihep.ac.cn

ABSTRACT: The Beijing Electron Positron Collider II upgrade (BEP-CII-U) has been proposed to optimize the maximum collision energy and data acquisition efficiency in higher energy region (> 2.1 GeV). To achieve higher luminosity at higher energies, the number of superconducting radio frequency (SRF) cavities will be doubled. The cryogenic system of the BEP-CII-U employs two cryogenic plants to provide the refrigeration for the three types of superconducting (SC) devices: SRF cavities, SC multi-function magnets (MFMs) and superconducting solenoid magnet (SSM). The cryogenic subsystem for SRF cavities has been upgraded from the original 500 W to 1 kW at 4.2 K due to the increased number of SRF cavities (4 cavities). The main tasks include the design of the cooling process, 499.8 MHz cavity cryomodules, local distribution valve boxes (LDVBs) and different types of multi-channel transfer lines (MCTLs) based on existing conditions. Meanwhile, the cryogenic subsystem for SC magnets has also been upgraded to enhance the reliability of the cryo-plant and to develop new SC MFM-cryomodules and associated valve boxes. The main tasks are including the design of the SC MFM-cryomodules, a cryogenic horizontal test stand (HTS) for SC magnets and working scheme for the main screw compressors (MSCs). The cryogenic system for the BEP-CII-U has been designed, constructed and commissioned since the beginning of 2021, and the detailed design is presented in this paper.

KEYWORDS: Accelerator Subsystems and Technologies; Acceleration cavities and superconducting magnets (high-temperature superconductor, radiation hardened magnets, normal-conducting, permanent magnet devices, wigglers and undulators); Gas systems and purification

*Corresponding author.

Contents

| | | |
|----------|---|-----------|
| 1 | Introduction | 1 |
| 2 | Upgrade principles of overall cryogenic system | 2 |
| 2.1 | Working scheme of main screw compressors | 2 |
| 2.2 | Usage and modifying measures of the main distribution valve box | 3 |
| 2.3 | Distribution design of cryogenic fluids for SRF cavities | 3 |
| 3 | Design of cryogenic subsystem for the SRF cavities | 4 |
| 3.1 | Main equipment and heat loads estimation | 4 |
| 3.2 | Cooling requirements and cooling process | 7 |
| 3.3 | Layout of cryogenic subsystem for the SRF cavities | 8 |
| 4 | Testing of cryogenic subsystem for the SRF cavities | 9 |
| 4.1 | Horizontal testing of the cryomodule in the cryogenic environment | 9 |
| 4.2 | Cooling down of the four cryomodules from 300 K to 4.2 K | 10 |
| 4.3 | Thermal stability of the cryomodules operation with RF power | 11 |
| 5 | Design of cryogenic subsystem for superconducting magnets | 12 |
| 5.1 | Cooling requirements and cooling process | 12 |
| 5.2 | Design optimization and heat load estimation for the SC MFM | 14 |
| 6 | Testing of the cryogenic subsystem for the SC magnets | 15 |
| 7 | Conclusion | 17 |

1 Introduction

The Beijing Electron Positron Collider II (BEPCII) is a double-ring collider that has been operating in the tau-charm energy region since the middle of 2007, and has achieved a series of significant results over the past nearly two decades [1]. Three types of superconducting (SC) devices are to be cooled by two separate cryogenic plant with the capacity of 500 W at 4.2 K temperature level. One cryogenic plant is cooling a pair of superconducting radio frequency (SRF) cavities located at the second interaction region (IR), while the other cryogenic plant is cooling a pair of superconducting multi-function magnets (MFMs) and a superconducting solenoid magnet (SSM) located at the first IR.

To enable more important physics studies in the energy region above 2.1 GeV and to maintain competitiveness in high-energy physics research, an urgent upgrade of BEPCII is required. The BEPCII upgrade (BEPCII-U) has been proposed to enhance the efficiency of collision data acquisition above 2.1 GeV and to increase the luminosity at the optimized energy of 2.35 GeV from 3.5×10^{32} to $1.1 \times 10^{33} \text{ cm}^{-2} \text{ s}^{-1}$. This improvement necessitates upgrading the radio frequency (RF) system from one to two cavities per ring, significantly raising the accelerating voltage [2]. To meet the cooling requirements of SRF cavities for the BEPCII-U, the corresponding cryogenic subsystem should be upgraded to a higher capacity due to the increased in the number of cavities (four in total). Meanwhile,

the new cryostats and horizontal test stand (HTS) for SC MFMs should be designed and constructed due to domestically development of the SC MFMs [3].

Therefore, the cryogenic subsystems for both the SRF cavities and SC magnets should be upgraded to meet new cooling requirements of SC devices based on the principle of maximizing the utilization of existing resources. The cryogenic system for BEPCII-U has been designed, constructed and commissioned since the beginning of 2021, and was put into operation and beam commissioning in March 2025.

2 Upgrade principles of overall cryogenic system

2.1 Working scheme of main screw compressors

The BEPCII cryogenic system should be operating continuously for approximately 10 months each year, that requires high reliability of the equipment. The main screw compressor (MSC), which increases the helium gas pressure in the cryogenic system, is a key rotating equipment with the highest failure rate in the cryogenic system. Moreover, restoring operation after a compressor shutdown requires considerable time, which is significantly influence on the overall operating reliability of the cryogenic system.

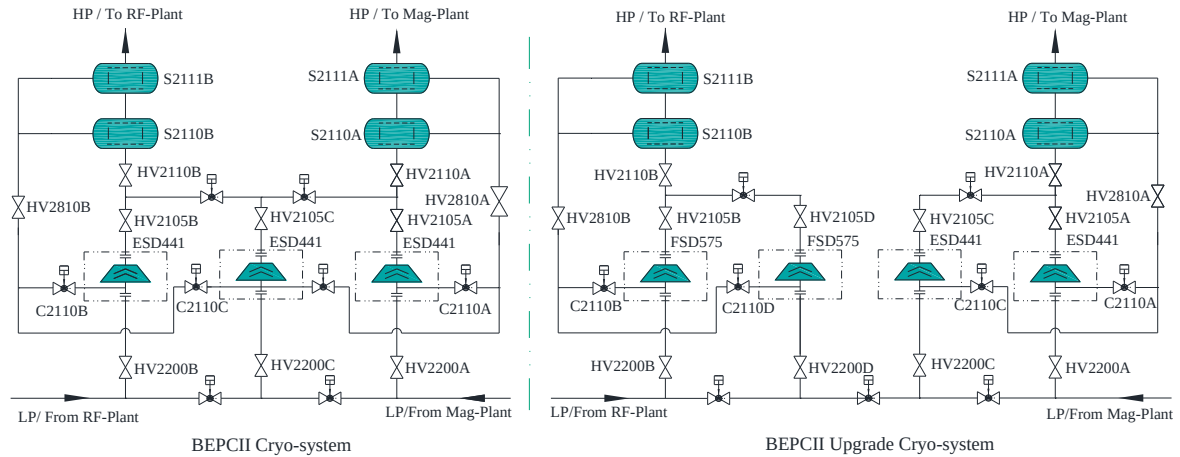


Figure 1. Working scheme of compressors in BEPCII and BEPCII-U.

In the BEPCII, two sets of refrigerators (Linde TCF50) with capacity of 500 W at 4.2 K are adopted to cool the superconducting facilities, and each refrigerator is equipped with the compressor of Caesar ESD 441, meanwhile, two refrigerators are sharing one spare compressor which can achieve a working scheme of two-using and one-standby. In the BEPCII-U, in order to improve the reliability of the cryogenic system and make full usage of existing equipment, two existing ESD 441 compressors are used together with a working scheme of one-using and one-standby in the cryogenic subsystem for SC magnets. Meanwhile, the cryogenic subsystem for the SC cavities should be upgraded to larger scale, two new FSD 575 compressors will be used together with a working scheme of one-using and one-standby in the cryogenic subsystem for the SRF cavities. The working scheme of the MSCs in the cryogenic system for the BEPCII and BEPCII-U are shown as figure 1.

Two MSCs are employed together with a working scheme of one-using and one-standby in each cryogenic subsystem, and the control strategies have been implemented as following: the SIGMA controllers of both MSCs are connected to PLC via Profibus-DP, and all of process signals from two

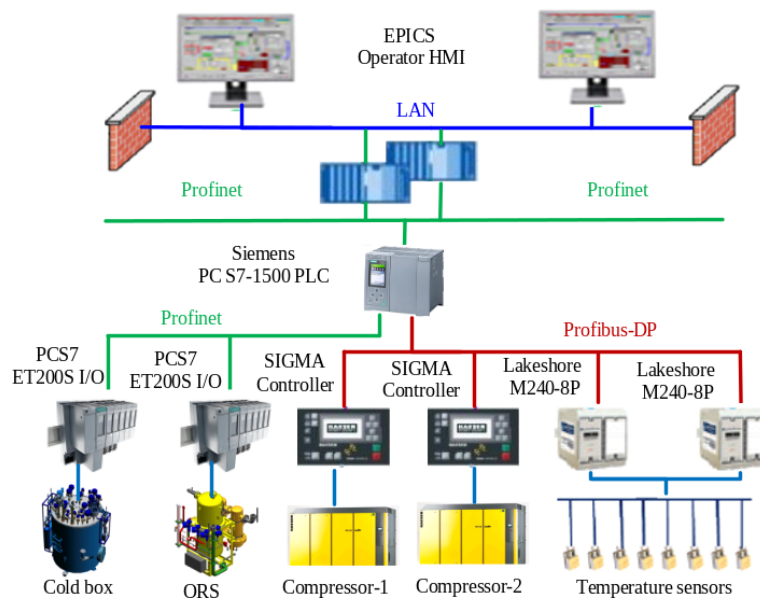


Figure 2. Simplified control scheme of two main compressors in the refrigerator system.

MSCs are integrated into the PLC, while both two SIGMA controllers of the MSCs should remain powered ON, but only one MSC is selected to run at any given time. The simplified control scheme for the two main compressors in the refrigerator system is shown as figure 2.

2.2 Usage and modifying measures of the main distribution valve box

The main distribution valve box (MDVB) is a complicated device in the BEPCII cryogenic subsystem for the SRF cavities, responsible for distributing and controlling cryogenic fluids to operating cryomodules and HTS for the cavities. The vacuum vessel of the MDVB is constructed from 316L stainless steel, which has a standard diameter of 1400 mm, a wall thickness of 10 mm and an overall length of 3952 mm. It houses twenty-four cryogenic valves, twenty-two cryogenic bayonets, twelve safety relief valves and various instrumentation [4]. The configuration of the MDVB is shown as figure 3. For the BEPCII-U, in order to maximize the use of existing equipment and reduce costs, the MDVB will be retained with modifications to certain cryogenic piping inside the vacuum vessel. Additionally, a new cooling process has been designed based on the existing piping and instrumentation diagram (P&ID) of the MDVB.

2.3 Distribution design of cryogenic fluids for SRF cavities

The design of the cooling process should comply with the following boundary conditions. Firstly, the two original 499.8 MHz cavity cryomodules will be retained, and two new 499.8 MHz cavity cryomodules of identical configuration will be added. Secondly, the cryogenic plant for SRF cavities will be upgraded to a higher refrigeration capacity in response to the increase from two to four cavities under BEPCII-U operational requirements. Thirdly, two new MSCs of Caesar FSD 575 compressors will be added and operated together with a working scheme of one-using and one-standby. Finally, the existing MDVB will be retained with modifications to the diameter of the internal cryogenic piping inside the vacuum vessel, and the HTS for the cavity testing under cryogenic conditions will also be kept in service.

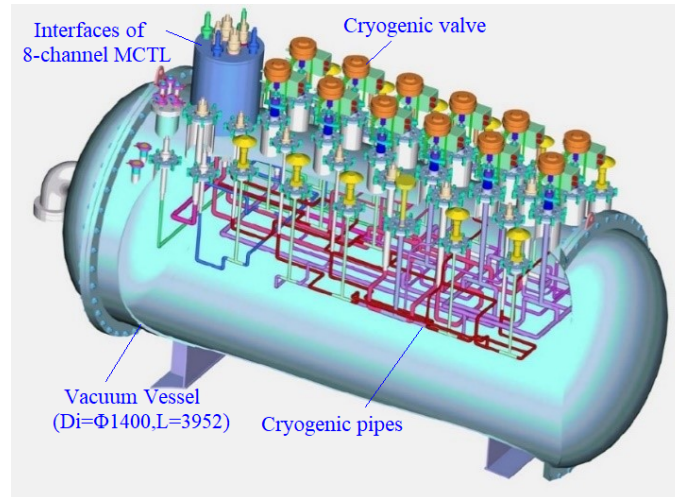


Figure 3. Configuration of the main distribution valve box.

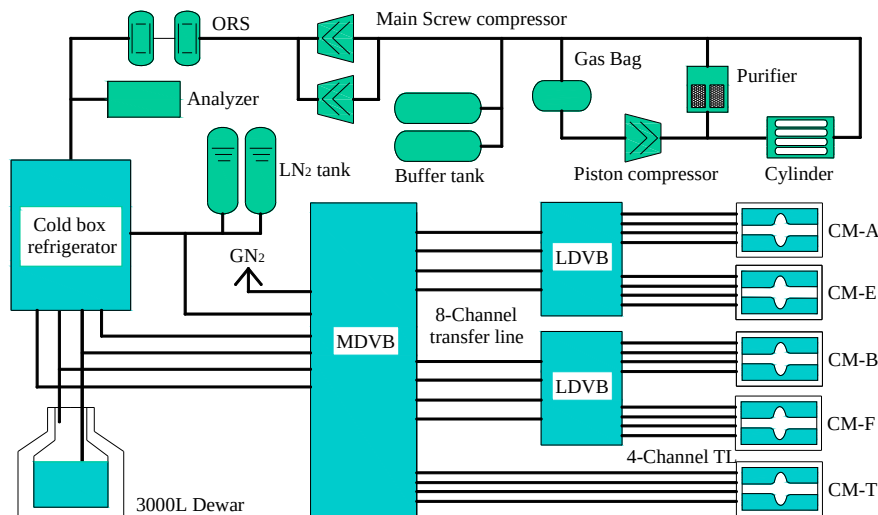


Figure 4. Block diagram of cryogenic subsystem for the SRF cavities.

Accordingly, the new cooling process for the SRF cavities is designed based on the existing MDVB. Two LDVBs will be added to re-distribute the cryogenic fluids, with one LDVB serving the two cavity cryomodules located each side. Two types of multi-channel transfer lines (MCTLs) will be located: one set between the MDVB and the LDVBs, and another set between each LDVB and corresponding pair of cavity cryomodules, respectively. A block diagram of the cryogenic subsystem for the SRF cavities is presented in figure 4.

3 Design of cryogenic subsystem for the SRF cavities

3.1 Main equipment and heat loads estimation

From the cryogenic point of view, the heat loads at various temperature levels are determined by the capacity and budget of the helium cryogenic system. The cryogenic subsystem for the SRF cavities is mainly consists of the cold box of a refrigerator, an LHe storage Dewar, four cavity cryomodules,

distribution valve boxes and different multi-channel cryogenic transfer lines, etc. Therefore, the thermal analysis of main contributors should be performed by finite element method (FEM) simulation to determine the heat loads at the 4.2 K temperature level.

According to block diagram (figure 4), the main equipment will be involved in the cryogenic subsystem for the SRF cavities, and two 499.8 MHz-cavity cryomodules, two LDVBs and different types of MCTLs should be added and designed. The layout of cryogenic subsystem for the SRF cavities, located at the second collider site of BEPCII, is shown in figure 5.

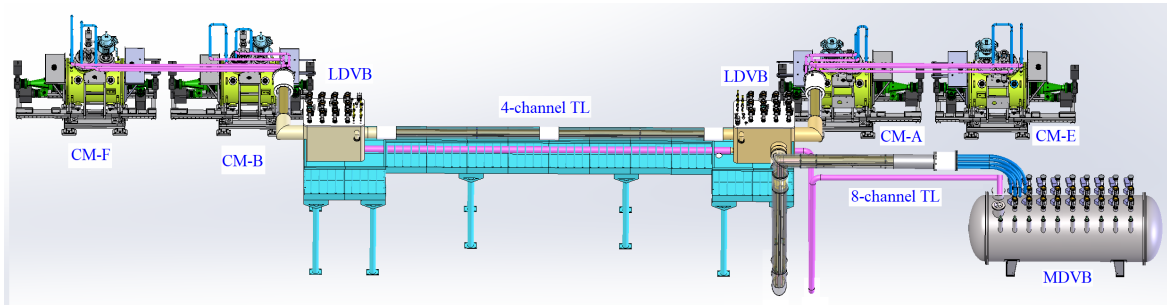


Figure 5. Layout of cryogenic subsystem for the SRF cavities at second collider site.

The 499.8 MHz single-cell cavities, which are derived from KEKB 508 MHz cavity and developed to the specifications of the BEPCII, have been adopted to replenish energy loss of the electron beam caused by photon radiation in the storage ring of the BEPCII. In the 499.8 MHz cavity cryomodule, the cavity is placed in vacuum-insulated cryostat with a liquid nitrogen thermal shield, and the cavity is immersed in a 4.5 K liquid helium bath to maintain superconductivity in a helium vessel of approximately 290 liters. The vacuum vessel with the standard diameter of 1000 mm, is constructed from pure iron and electroplated with Zinc to minimize the ambient magnetic field. The thermal shield with oxygen-free high-conductivity (OFHC) copper is cooled by liquid nitrogen (LN_2) and covered by 50 layers of multi-layer insulation (MLI) to reduce the radiation heat load. Due to the pressure sensitivity of the SRF cavity frequency, a piezoelectric tuner is used to compensate for the frequency excursion by adjusting the cavity length. Given the limited range of the tuner, pressure fluctuations in the helium vessel should be controlled within ± 3 mbar. A fixed-coupling coupler with 150 kW continuous-wave (CW) travelling-wave power is employed, and out conductor and inner conductor of power coupler are cooled by helium gas and cooling water, respectively [5]. The configuration of the 499.8 MHz cavity cryomodule is shown in figure 6(a).

Steady-state thermal analysis of 499.8 MHz cavity cryomodule was performed using the ANSYS software under the following boundary conditions, the temperature of vacuum vessel, the tubes of thermal shield and helium vessel were set at 300 K, 80 K and 4.2 K, respectively. The calculated static heat loads at 4.2 K temperature level is about 17 W by the FEM simulation, and the resulting temperature distributions are obtained and shown in figure 6(b).

The LDVBs and different types of MCTLs were designed to re-distribute the cryogenic fluids while incorporating vacuum barriers within the MCTLs to maintain independent the respective insulation vacuum. The steady-state thermal analysis of the MCTLs was also performed by the ANSYS software applying the same boundary conditions, the temperature of vacuum vessel, cryogenic pipes of thermal shield and helium cryogenic pipes are 300 K, 80 K and 4.2 K, respectively. The temperature distributions are obtained by the FEM simulation and shown in figure 7.

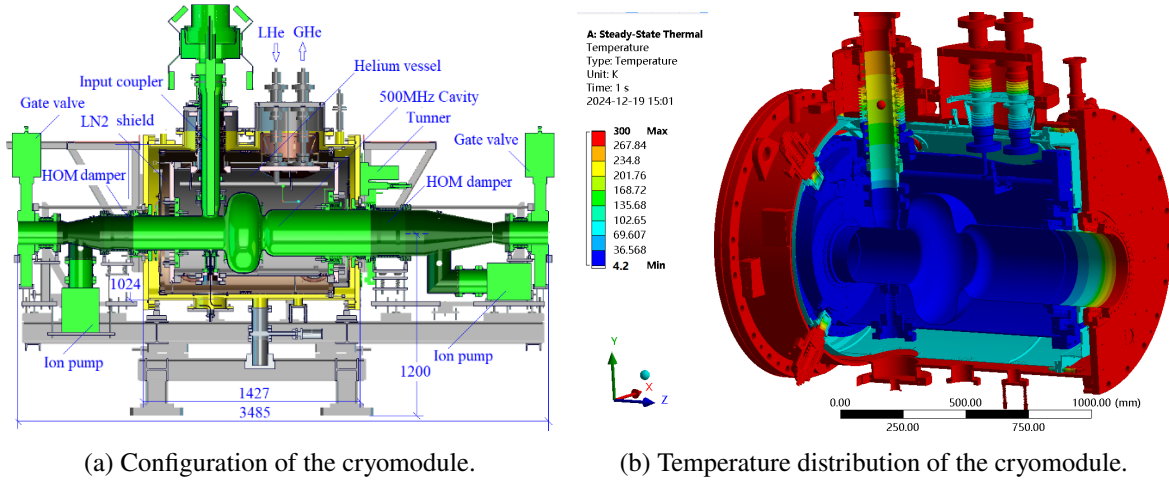


Figure 6. Configuration and thermal analysis of the 499.8 MHz cavity cryomodule.

For the cryogenic valves and cryogenic bayonets, the heat load is estimated at 1 W per unit. The calculated heat loads at 4.2 K temperature level are 0.48 W/m for eight-channel transfer line and 0.30 W/m for four-channel transfer line. To be conservative in the design, a uniform value of 1 W/m at 4.2 K temperature level is adopted for the different multi-channel transfer lines, which are taken into account in the overall heat loads estimation at the 4.2 K temperature level.

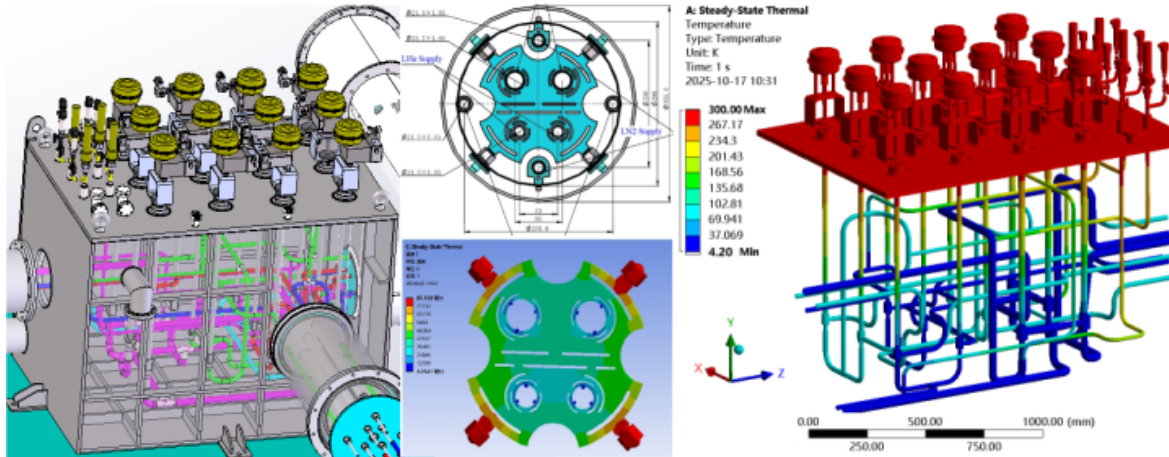


Figure 7. Configuration and thermal analysis of the LDVBs and MCTLs.

The dynamic heat load (P_{cav}) of superconducting cavity is expressed as following equation, and calculated dynamic heat load is 57.1 W.

$$P_{cav} = \frac{V_{acc}^2}{(R_s/Q_s)Q_0} \quad (3.1)$$

Where, V_{acc} is the accelerating voltage in the field, $V_{acc} = 1.65$ MV [2]; Q_0 is the intrinsic quality factor of the resonance cavity, $Q_0 = 5 \times 10^8$; R_s/Q_s is the shunt impedance of the cavity, $R_s/Q_s = 95.3 \Omega$ [6].

The total heat loads of the main contributors determines the required refrigeration capacity of the helium refrigerator. However, a discrepancy between the design values and the actual performance

of components should be inevitable for the large-scale cryogenic system. Therefore, to mitigate construction risk, the actual refrigeration capacity is typically specified to be larger than the calculated demand. The estimated heat loads at 4.2 K for the cryogenic subsystem serving the SRF cavities are summarized in table 1.

Table 1. Estimation heat loads at 4.2 K in the cryogenic subsystem for SRF cavities.

| Heat source | Quantity | Heat load/W |
|---|----------|---------------------|
| Static heat load of cryomodules | 4 | $4 \times 50 = 200$ |
| Dynamic heat load for cavities | 4 | $4 \times 57 = 228$ |
| Dynamic heat load for couplers | 4 | $4 \times 5 = 20$ |
| Main distribution valve boxes(MDVBs) | 1 | $1 \times 50 = 50$ |
| Local distribution valve boxes(LDVBs) | 2 | $2 \times 20 = 40$ |
| Cryogenic transfer line and vacuum barriers | 60 m | $60 \times 1 = 60$ |
| 3000L LHe storage Dewar and heater | 1 | $1 \times 70 = 70$ |
| Margin | 20% | 133.6 |
| Summary | | 801.6 |

3.2 Cooling requirements and cooling process

The total estimated heat loads at 4.2 K temperature level is approximately 802 W, it is as summarized in table 1, therefore, the cooling capacity of the refrigerator has been selected as 1 kW at 4.2 K temperature level to meet the operational requirements of four SRF cavities. This refrigerator system includes a cold box, main screw compressors and 3000-litter LHe Dewar.

A helium refrigerator with the capacity of 1 kW@4.2 K based on the modified Claude cycle with liquid nitrogen precooling has been adopted, and cooling process diagram of the refrigerator is designed by Air Liquide company. The low-pressure helium gas from the buffer tank is compressed to 1.45 MPa by the MSC of KAESER FSD 575, and the high-pressure helium gas is entered the cold box of refrigerator, where it is cooled to about 80 K in plate-fin heat exchangers of the HE1 and HE2 by counter flow with liquid nitrogen and low-pressure return helium gas. After passing through an 80 K absorber to remove impurities (e.g., N_2 , O_2 , C_xH_y), the helium is further cooled in HE3 and then splits into two streams: a turbine stream and a Joule-Thomson (JT) stream. The turbine stream expands through a first-stage turbine, passes through HE4, expands again in a second-stage turbine, and finally mixes with the low-pressure return gas. The JT stream is cooled sequentially in HE4, HE5, and HE6 before entering a 20 K absorber to remove impurities such as neon and hydrogen. After further cooling in HE7 and HE8, the supercritical helium is throttled through a JT valve to produce liquid helium.

The cold box provides three output streams: supercritical helium output, a 40–300 K mixture gas output, and a two-phase helium output. The refrigerator operates in three modes: refrigeration mode, liquefaction mode and mixed mode, and its specified refrigeration performances includes a capacity of 1000 W @ 4.2 K in refrigeration mode and 280 L/h in liquefaction mode with liquid nitrogen precooling.

The cooldown procedure for the four cavity cryomodules is described as following, initially, the cryomodules are cooled using a 40–300 K mixture gas from the cold box of the refrigerator, and when the temperatures of cavities reach about 40 K, the supply line is switched from the cold box to the LHe

storage Dewar until the cavities are immersed in the 4.2 K liquid helium. Meanwhile, the dedicated cooldown and warmup pipelines have been incorporated into the transfer line to ensure operational independence of the four cavities, and this design allows any cryomodule to be cooled down or warmed up without disrupting the cryogenic state of others. In other words, if a cryomodule requires maintain, it can be warmed up and subsequently re-cooled without affecting the operation of remaining cryomodules. A simplified flow chart of the cryogenic system for SRF cavities is shown in figure 8.

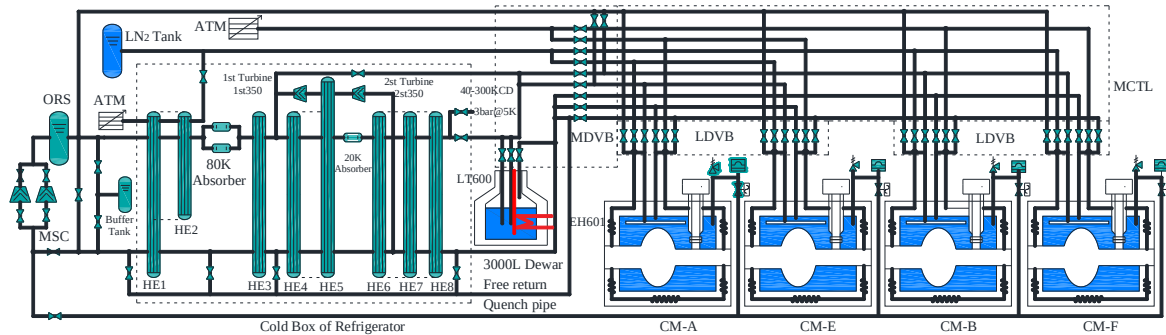


Figure 8. Simplified flow chart of the cryogenic system for the SRF cavities.

When a quench happens occasionally in the cavities, a substantial amount of heat will be released into liquid helium which may lead to overpressure in the helium vessel. From a cryogenic perspective, a quench pipe is connected to the suction side of the main compressor to help manage the released gas. Additionally, a three-stage pressure protection system is implemented to prevent overpressure in the helium vessel. This safety devices system consists of an electrically activated safety valve set at 1.26 bara, a mechanical relief valve set at 1.30 bara and a rupture disk rated at 1.98 bara. Helium gas discharged through relief valve is vented to the atmosphere outside of the tunnel, and the helium gas is released directly into the tunnel in the case where the rupture disk bursts [7].

3.3 Layout of cryogenic subsystem for the SRF cavities

There are three types of superconducting facilities in the BEPCII-U, two pairs of SRF cavities, one pair of interaction region SC MFMs and one detector solenoid superconducting magnet (SSM). The SSM and a pair of SC MFMs are located in the first colliding hall, while two pairs of SRF cavities are located in the second colliding hall. Two separate helium refrigerators are employed to meet the cooling requirements of superconducting devices. The cryogenic system infrastructure is distributed across several areas, including the first colliding cryo-hall, the second colliding cryo-hall, the compressor hall, the recovery hall and helium gas storage tank farm. The overall layout of the cryogenic system for the BEPCII-U is shown as figure 9.

In the BEPCII-U, the functional zones of cryogenic system are retained, while layout of the cryogenic subsystem for the SRF cavities has been redesigned, involving the second colliding hall and compressor hall. The second colliding hall houses a cold box of the 1 kW@4.2 K refrigerator, 3000-litter LHe storage Dewar, the MDVB and the cabinets of relevant secondary instrumentation associated with process controller. The compressor hall accommodates four MSCs, two oil removal system (ORSs) and gas managing devices, all of which are subject to factors such as vibration, noise and maintenance activities.

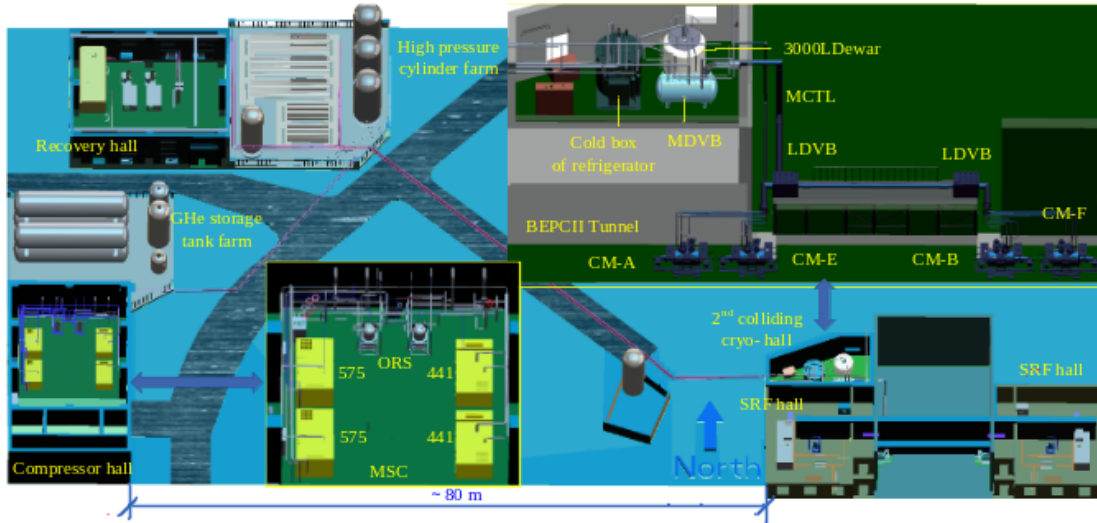


Figure 9. Layout of the cryogenic system for the BEPCII-U.

The two compressors for the each cryogenic plant, which operating pressure is between an inlet pressure of 1.05 bar and an outlet pressure of 14.5 bar, are installed together in compressor hall. Each set of ORS is located downstream of compressor outlet, which employs multi-stage coalescing filters and composite material filters to ensure that the residual oil content in the high-pressure helium gas does not exceed 10 ppb. The purification and recycling equipment with a purification ability of $105 \text{ m}^3/\text{h}$ and a working pressure of 20 MPa, which is situated in the recycling hall. This system includes the recovery piston compressors, a cryogenic purifier, an impure-gas rubber bag and related ancillary facilities. The cryogenic purifier uses activated carbon in the liquid nitrogen environment to remove contaminants at high pressure of 20 MPa, achieving a helium purity exceeding 99.9995% after purification [8] Additionally, the pressure vessels are located outdoors in the storage farm, these comprise medium-pressure helium storage tanks (130 m^3 each), high pressure cylinders (26 m^3 per unit) and liquid nitrogen storage tanks (30 m^3 each).

4 Testing of cryogenic subsystem for the SRF cavities

4.1 Horizontal testing of the cryomodule in the cryogenic environment

The 499.8 MHz cavity cryomodule has been constructed and tested in the HTS located at Platform of Advanced Photon Source Technology R&D (PAPS), and the horizontal test of the cryomodule in the cryogenic environment aims to verify the proper operation behavior of the cavity and associated components under nominal working conditions, as well as to measure both the static and RF-induced dynamic heat loads in the liquid helium environment [9]. Each cryomodule is tested under cryogenic conditions similar to those in the actual accelerator tunnel before being put into the operation for the beam commissioning. The view of the cryomodule installed in HTS is shown in figure 10.

Two measurement methodologies are typically employed to determine heat loads at 4.2 K temperature level, which are including flowmeter method and level-meter method, these can be written as eqs. (4.1a) and (4.1b) [10]. In the flowmeter method, the heat load to the liquid helium circuit

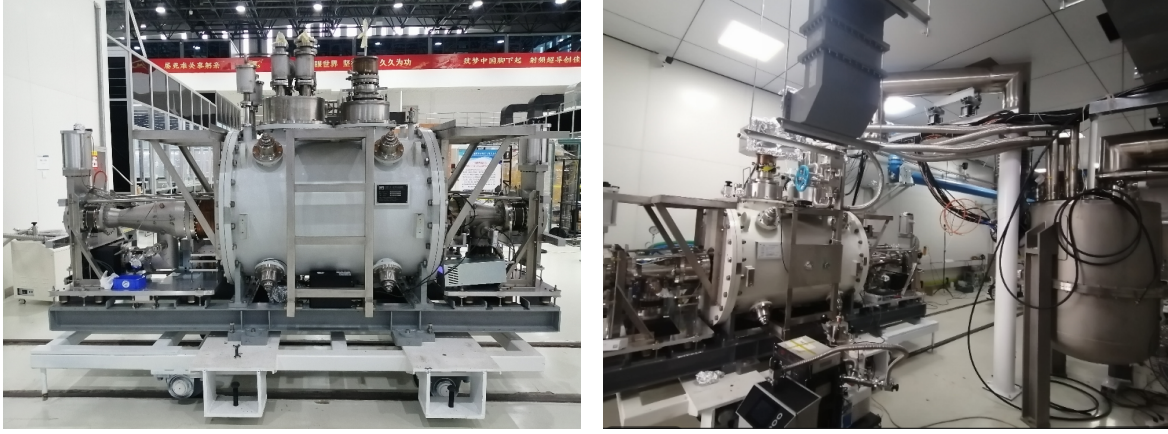


Figure 10. 499.8 MHz cavity cryomodule in the HTS.

is calculated from direct measurements of the GHe mass flow rate. In the level-meter method, it is derived from the rate of LHe level drop by level gauge. In both cases, the total heat deposited into the liquid helium is evaluated by multiplying the vaporized helium by the latent heat of helium at the operating temperature.

$$Q_{\text{static,FI}} = \dot{m}_{\text{GHe}} \gamma_{\text{He}} \quad (4.1a)$$

$$Q_{\text{static,LI}} = \frac{\Delta L}{\Delta t} A_{\text{hv}} \rho_{\text{LHe}} \gamma_{\text{He}} \quad (4.1b)$$

Where, $Q_{\text{static,FI}}$, $Q_{\text{static,LI}}$ are the calculated heat load by the method of the flowmeter and the level-meter, respectively, W; \dot{m}_{GHe} is the mass flow rate of vaporized GHe, g/s; γ_{He} is the latent heat of LHe, J/g, $\gamma_{\text{He}} = 20.14\text{J/g}$ [11]; ΔL is the level drop of LHe, cm; A_{hv} is the cross-sectional area of the helium vessel, cm^2 ; Δt is the measurement duration, s; ρ_{LHe} is the density of LHe, g/cm^3 .

During the heat load experimental measurement, the LHe supply to the bath should be stopped by closing valve CV6710 and return GHe stream should be completely discharged. The LHe level was allowed to drop from 98% to 90% (an 8% decrease), and the trend curves of relevant operational parameters during the test are shown as figure 11. The curves indicate that each parameter gradually stabilized over the measurement period. The mass flow rates settled slowly, and time-integrated averages over a steady interval were used for the heat-load calculations. Based on the data in figure 11 and the above expressions, the measured heat loads can be calculated and summarized in the table 2. The measured static heat loads by the flow meter method and level meter method are obtained as 26.11 W and 29.58 W by the experimental data, respectively, and the results by two methods can be checked each other. The static heat loads measured by the two methods show a slight discrepancy. The result obtained from the mass flow rate method is considered relatively more accurate, whereas the result derived from the level-meter method may be influenced by the geometry of the helium vessel.

4.2 Cooling down of the four cryomodules from 300 K to 4.2 K

Four 499.8 MHz cavity cryomodules have been installed in the tunnel of BEPCII storage ring and subsequently integrated into the accelerator system, including radio-frequency and cryogenic distribution networks. The cooling requirements for each cryomodule are as follows, insulation vacuum of the cryostat and beam vacuum of the cavity shall be better than 10^{-3} Pa and 10^{-7} Pa at

Table 2. Measured heat load with experimental data.

| Item | Time (hh:mm:ss) | ΔL /(%) | $\rho_{\text{LHe}}/(g/l)$ | $\Delta t/(s)$ | $\bar{m}_{\text{He}}/(g/s)$ | $Q_{\text{static,LI}}/(W)$ | $Q_{\text{static,FI}}/(W)$ |
|-------|--------------------|--------------------|---------------------------|----------------|-----------------------------|----------------------------|----------------------------|
| Value | 11:22:18–11:39:00 | 8 | 121.1 | 1002 | 1.2963 | 29.58 | 26.11 |

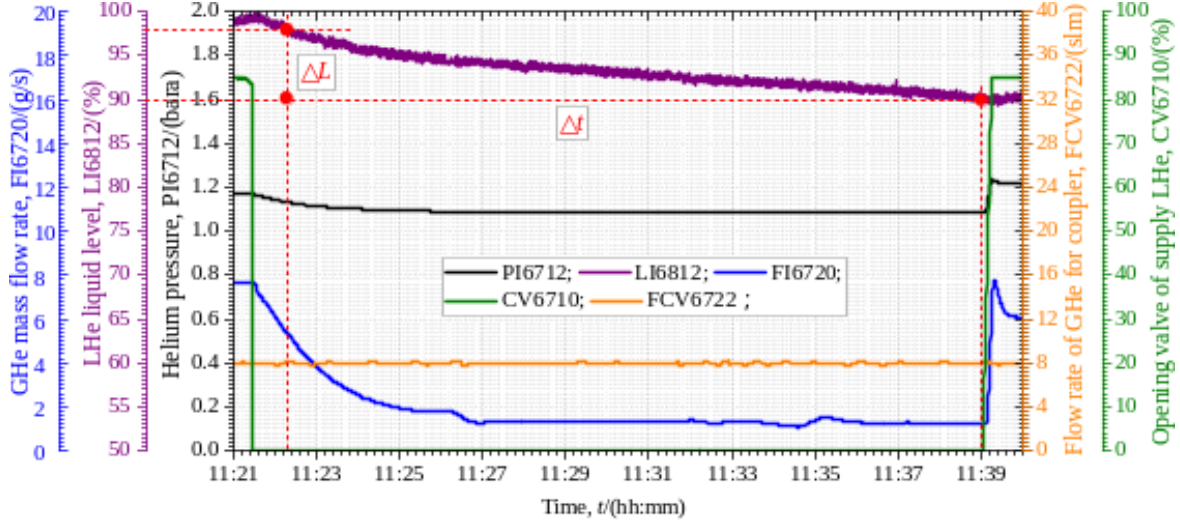


Figure 11. Trend curves of operational parameters in the static heat load experiment.

the room temperature, respectively, maximum temperature difference between any two temperatures point inside the helium vessel is limited to 10 K, and maximum cooling rate for a given temperature point is controlled within 5 K/hour [10].

The successful cooling down of the four cryomodules from room temperature to 4.2 K have been carried out in the May and August 2025. During the cooling process, the 80 K thermal shield circuit was first cooled down using the liquid nitrogen supplied from the LN₂ storage tank, and the 4 K circuit was then cooled down by a mixture of 40 K and 300 K helium gas from the cold box of the refrigerator. When the temperatures of dressed cavity reached approximately 40 K, the helium supply was switched from cold box to LHe storage Dewar, cooling continued until the cavity was completely immersed in a 4.2 K liquid helium bath and the target level was reached, marking the completion of cooldown process. The entire cooling process lasted approximately 3.5 days, and the cool down curves of cryomodules are shown in figure 12.

4.3 Thermal stability of the cryomodules operation with RF power

There are requirements for the helium pressure and LHe level fluctuations in the helium vessel of the cryomodule in the RF-powered operation to remain within ± 3 mbar and $\pm 1\%$, respectively. The automatically control strategies have been implemented to ensure the thermal stability of the cryomodule in the cryogenic system are as follows: the valve opening on the supply line is interlock controlled with the LHe level measured by LI2400, the dynamic heat load of cavity is regulated by interlocking with the power of an electrical heater, meanwhile, the cooling gas flow rate for the power coupler is maintained at 8 slm (standard liter per minute, slm) by the flow-control valve FCV2400.

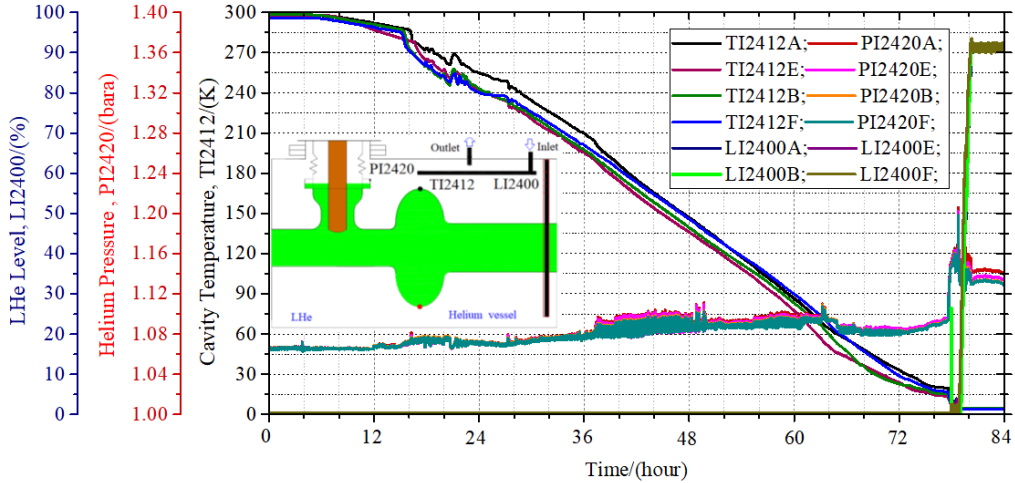


Figure 12. Cool down curves of four cryomodules from 300 K to 4.2 K.

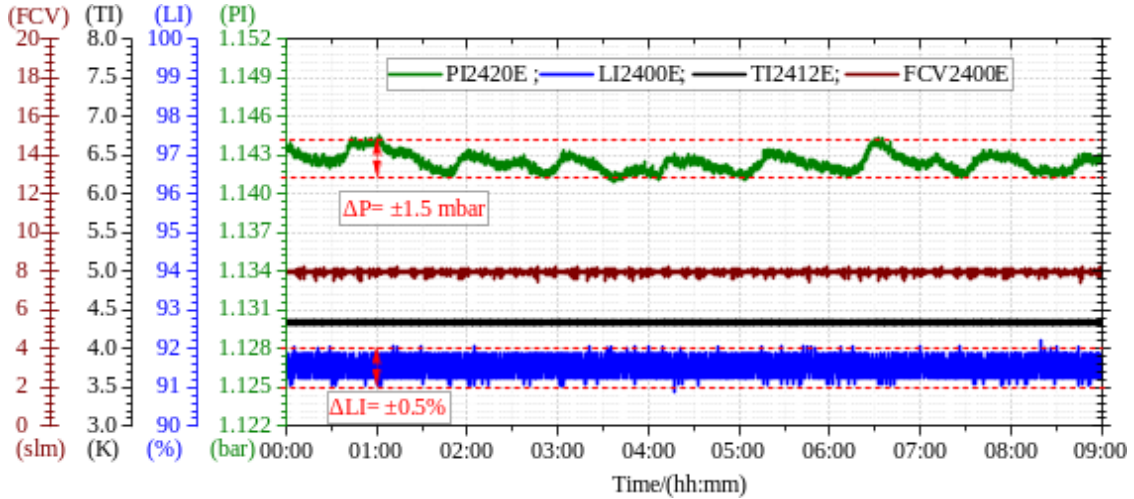
In order to verify the thermal stability of the cryomodule in the operating conditions, each cavity is continuously conditioned with an accelerating voltage for a long time. One cavity per ring was selected and conditioned with RF power to meet requirements of initial commissioning, and cavity-E and cavity-B are operated at an accelerating voltage of 1.5 MV for 9 hour. Steady-state trends of operational parameters are shown as figure 13. It can be seen from figure, when the cavity is loaded with the accelerating voltage of 1.5 MV, the operation parameters including the helium pressure of PI2420 and LHe level of LI2400 in helium vessel were stable, and the fluctuations was controlled within ± 1.5 mbar and $\pm 0.5\%$ during the operation duration, respectively, which indicates that the measured results are well within the specified thermal-stability requirements.

5 Design of cryogenic subsystem for superconducting magnets

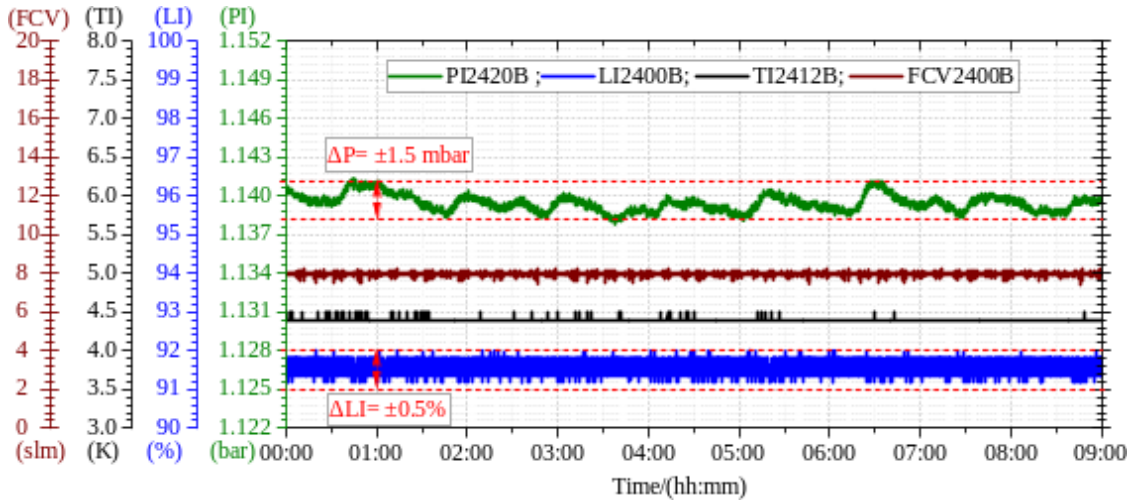
5.1 Cooling requirements and cooling process

In the BEPCII, a pair of a superconducting MFMs in the storage ring and a superconducting solenoid magnet (SSM) in the BESIII (Beijing spectrometer III) detector are installed in the first interaction region. These three types of superconducting magnets are cooled by a cryogenic plant based on the Linde TCF50S refrigerator, which provides a refrigeration capacity of 500 W at 4.2 K temperature level. The superconducting MFM was designed by Brookhaven National Laboratory (BNL) and Institute of High Energy Physics (IHEP), and fabricated at BNL superconducting magnet division during the BEPCII construction. It consists of different types of magnet coils: superconducting quadrupole (SCQ) with a serpentine coil structure, a bending dipole (SCB) or horizontal dipole coil (HDC), a vertical dipole coil (VDC), a skew quadrupole (SKQ), as well as three anti-solenoid (AS1, AS2, AS3) windings [12, 13].

For the BEPCII upgrade, there are three tasks should be performed in the cryogenic subsystem serving the SC magnets. Firstly, enhancing system reliability of the SC magnets cryo-plant, the two existing ESD 441 compressors will be operated together with a working scheme of one-using and one-standby to improve the cryogenic system reliability while maximizing the use of existing equipment. Secondly, developing new cryostats and valve boxes, a pair of cryostats and associated



(a) SRF Cavity-E



(b) SRF Cavity-B

Figure 13. Steady operational parameters of the cryomodules with RF power.

valve boxes for the SC MFMs have been designed and constructed based on the new MFM coils to meet the BEPCII-U requirements. Finally, building a new horizontal test stand (HTS), a cryogenic HTS for the SC magnet cryostats with the constrained cooling channels in the supercritical helium will be constructed to verify the performances of new SC magnets. Therefore, from a cryogenic perspective, the primary objectives are to improve the reliability of the SC magnets cryoplant and to develop and test the new SC MFM cryomodules and their valve boxes.

To avoid flow instabilities in the constrained cooling channels of the SC magnet cryostats, a subcooled helium flow scheme was employed. The cooling process proceeds as follows. High-pressure helium gas at 14.5 bar from the MSC flows enters the cold box of the refrigerator, and after undergoing a series of complex refrigeration stages, the fluid exits as supercritical single-phase helium at approximately 5 K and 2.7 bar. This supercritical helium is then subcooled using boiling saturated helium in a 1000-liter storage Dewar. The subcooled helium circulates through the cooling channel of the SC magnet cryomodule to remove the deposited heat, and then returns to the 1000-liter

storage Dewar. A control valve maintains the operating pressure below the critical point of the helium. Meanwhile, the branches of returning vaporized helium gas are used to cool the gas-cooling type of current leads, and the helium exiting at near room temperature. A simplified flow diagram of the cryogenic system for SC magnets is shown as figure 14.

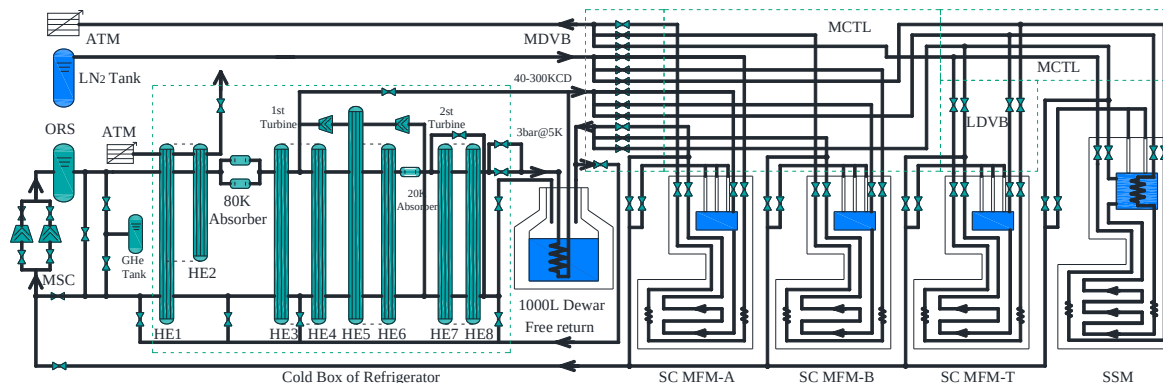


Figure 14. Simplified flow diagram of the cryogenic subsystem for the SC magnets.

5.2 Design optimization and heat load estimation for the SC MFM

The circumference of BEPCII storage ring is 238 m and the length of first interaction region (IR) is only about 14 m, and resulting in very tight spatial constraints for installation the magnet system [14]. Consequently, all equipment in first IR should be specially designed to fit within this limited tight space while meeting the requirements for high current intensity and large beam aperture. Two SC MFM cryomodules were inserted symmetrically in the BESIII detector relative to the interaction point, an assembly view of a cryomodule with its valve box in the first IR is shown as figure 15.

A new SC MFM coil based on BNL design scheme was developed and constructed domestically to increase the magnetic field gradient of central superconducting quadrupole (SCQ) from 18.7 T/m to 25 T/m, while retaining the performances of all other coils and maintaining the overall dimensions of the magnet [15]. Therefore, a pair of cryostats for the SC MFM have been developed and constructed to meet the BEPCII-U specifications, and the gas-cooling current leads with Bi2223 high-temperature superconducting for the SCQ and the associated AS coil are designed in the valve boxes [16], which this design also resolved pre-existing issues of vacuum leakage and frosting on the warm side of the current leads.

The superconducting wigglers (SCWs) were introduced approximately four decades ago and have since been widely employed at many synchrotron radiation (SR) facilities worldwide [17–20]. While the serpentine coil, which allows arbitrary multipolarity to be achieved in a single continuous winding process, is particularly well-suited for the interaction regions with stringent space constraints and high field requirements. Consequently, serpentine windings have been adopted in magnets for the BEPCII and J-PARC, and are proposed for compact final-focus magnets in the International Linear Collider (ILC) [14, 21, 22].

The cryostats for SC MFMs should be designed as compactly as possible, and the design optimization was performed to reduce the heat load by adjusting component dimensions based on the new magnet coils. The main components of SC MFM cryomodule from outer to inner are described as follows: outer vacuum shell, outer thermal shield, outer LHe shell, magnet coils, coil

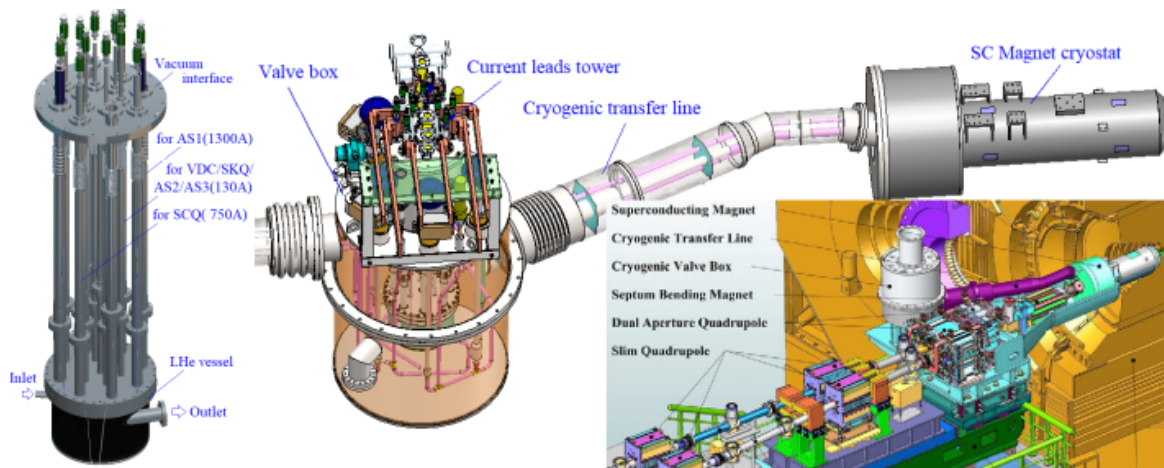


Figure 15. Assembly of SC magnet cryomodule and its valve box in the first IR.

support cylinder, inner LHe shell, inner thermal shield and inner vacuum shell. Meanwhile, eight radial Key-supports with G10 retainers for low thermal conductivity are fixed on the outer LHe shell, and the subcooled helium fluid flowing inside the LHe vessel removes the conductive and radiative heat [23]. The thermal shield, which is made from oxygen-free copper (OFC) and covered by the MLI, is cooled by LN₂ tubes to minimize the radiative heat load. The configuration of the SC magnet cryomodule is shown as figure 16.

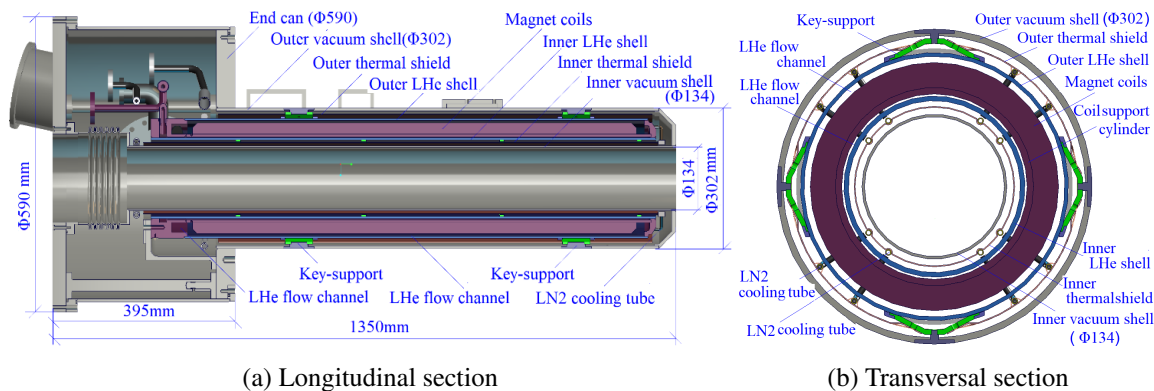


Figure 16. Configuration of the SC MFM cryomodule.

Steady-state thermal analysis is performed using the ANSYS software under the following boundary conditions, the temperature of vacuum vessel, the tubes of thermal shield and helium vessel were set at 300 K, 80 K and 4.2 K, respectively. The calculated static heat loads is approximately 16 W at 4.2 K temperature level by FEM simulation, and the resulting temperature distributions are shown in figure 17.

6 Testing of the cryogenic subsystem for the SC magnets

Each SC magnet cryomodule was assembled with its magnet coil and installed in the HTS which provides power supply, instrumentation and cryogenic cooling. The horizontal test of the SC magnet

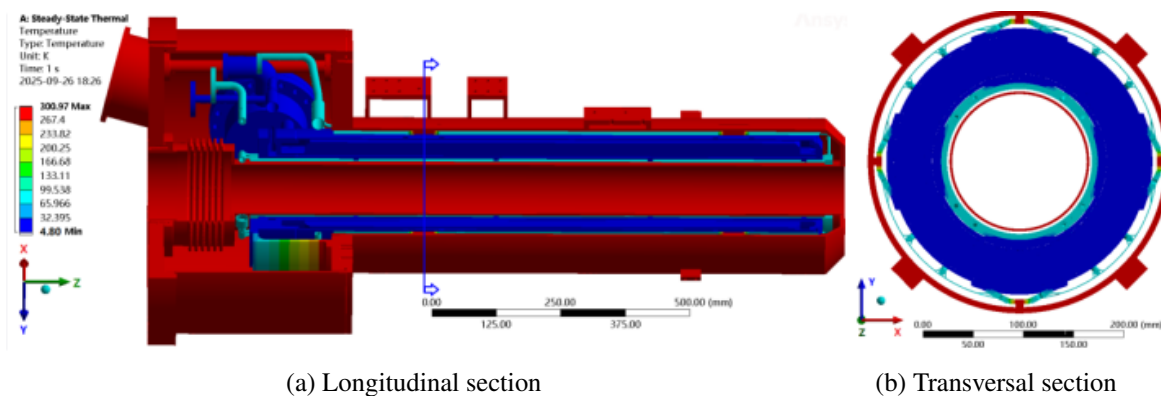


Figure 17. Temperature distribution of the SC MFM cryomodule.

cryomodule under the cryogenic conditions aims to verify the proper operation of the SC magnet and associated components under nominal working conditions, as well as to measure the static heat loads in a liquid helium environment. Each cryomodule is assembled and tested in the HTS where conditions simulate the actual cryogenic environment of accelerator tunnel, and then integrated into the formal accelerator system and put into operation. Photographs of the SC MFM magnet cryomodule installed in the HTS and subsequently in the BESIII detector are shown as figure 18.

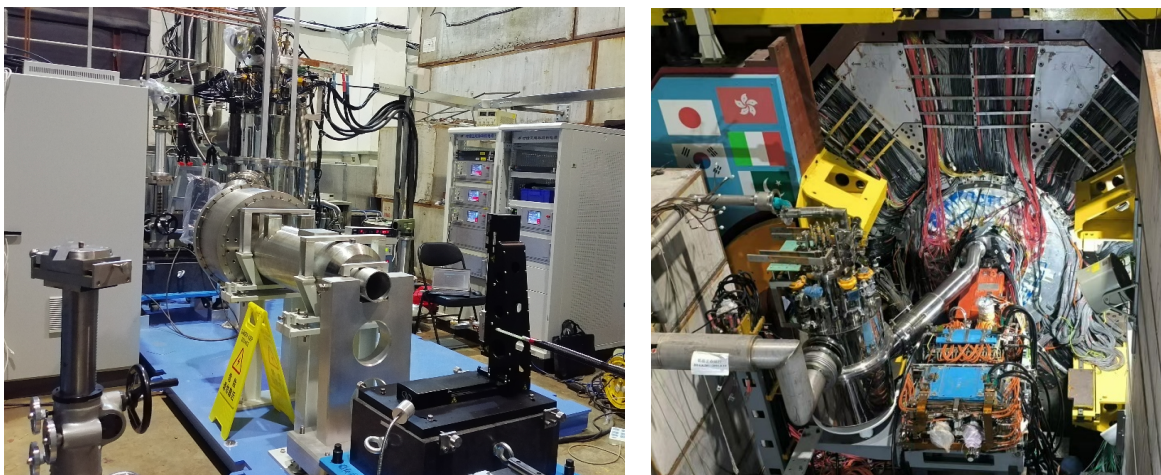


Figure 18. SC MFM magnet cryomodule in the HTS and BESIII detector.

The first successful cooldown of the SC MFM cryomodule from room temperature to 4.2 K was completed in August 2023. The cooling process should be performed slowly to prevent thermal stress and deformation of mechanical structure. Accordingly, the following requirements were imposed on the cooldown of the cold mass. The maximum cooling rate at any given temperature in the helium circuit should not exceed 5 K/hour, and the maximum temperature difference between any two points inside the helium shell should be limited to 10 K. The cooling process from 300 K to 4.2 K lasted approximately 84 hours, and the temperature trends of the cryomodule during the cooldown process are shown in figure 19.

Supercritical helium flows through the cooling channel of the cryostat to remove the deposited heat, and then return to the 1000-liter storage Dewar, and a control valve maintains the pressure

below the critical point of the helium. During the experimental measurement of heat load, operational parameters were continuously monitored and recorded to ensure the thermal stability throughout test.

The measurement methodologies were typically used to determine heat load at 4.8 K temperature level, which can be written he following expression eq. (6.1)

$$Q_{\text{static}} = \dot{m}_{\text{He}} [h_{\text{He,inlet}}(T_{\text{inlet}}, P_{\text{inlet}}) - h_{\text{He,outlet}}(T_{\text{outlet}}, P_{\text{outlet}})] \quad (6.1)$$

Where, Q_{static} is the static heat load, W; \dot{m}_{He} is the mass flow rate of GHe, g/s; $h_{\text{He,inlet}}$ $h_{\text{He,outlet}}$ are the specific enthalpies of helium at the inlet and outlet, which is determined from the measured temperature and pressure, J/g; T is the helium temperature, K; P is the helium pressure, bara.

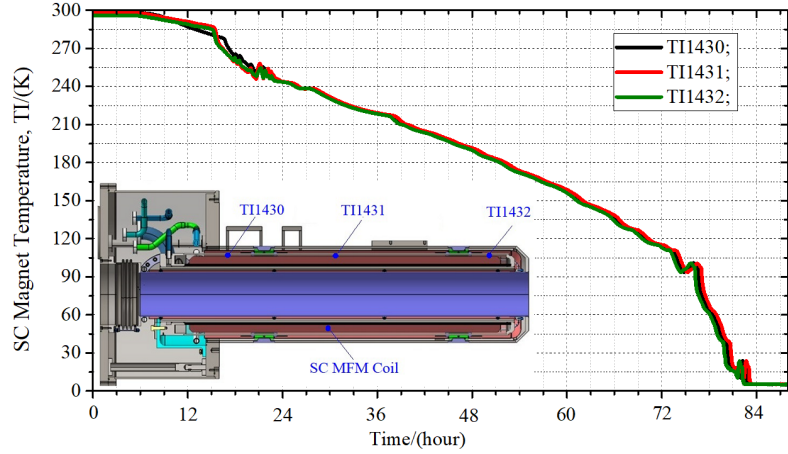


Figure 19. Cool down trends of cryomodule from 300 K to 4.2 K.

Steady-state operational parameters are monitored and measured in the cryogenic environment, and the measured heat load can be obtained as approximately 27.28 W according to eq. (6.1). Detailed experimental results are summarized in table 3.

Table 3. Measured heat load with experimental data.

| Item | \dot{m}_{He} /(g/s) | T_{inlet} /(K) | P_{inlet} /(K) | $h_{\text{He,inlet}}$ /(J/g) [11] | T_{outlet} /(K) | P_{outlet} /(K) | $h_{\text{He,outlet}}$ (J/g) [11] | Q_{static} /(W) |
|-------|---------------------------------|----------------------------|----------------------------|--------------------------------------|-----------------------------|-----------------------------|-----------------------------------|-----------------------------|
| Value | 7.60 | 4.89 | 1.45 | 32.984 | 5.31 | 1.43 | 36.574 | 27.284 |

The two new SC MFM cryomodules and their valve boxes are installed symmetrically in the BESIII detector with respect to the interaction point, and then integrated into the accelerator system, including both electromagnetic and cryogenic distribution networks. Successful cooldown of a pair of superconducting MFMs and a superconducting SSM from room temperature to 4.2 K have been achieved in the March and August 2025, after which the cryogenic subsystem for SC magnets has been put into cryogenic operation and beam commissioning for a long time.

7 Conclusion

The cryogenic system for the BEPCII Upgrade has been designed, constructed and commissioned from March 2021 to May 2025. In this project, the cryogenic subsystem for SRF cavities has been

upgraded from an original 500 W to 1 kW at 4.2 K to accommodate the increased number of cavities (from two to four), and the cooling process and main equipment for this subsystem were designed and implemented making full use of existing infrastructure. Simultaneously, the cryogenic subsystem for SC magnets was upgraded to improve the reliability of the cryoplant and to develop new SC MFM cryomodules and their associated valve boxes, and a dedicated HTS for the SC magnet cryomodule with the constrained cooling channels was also constructed to validate the performance of the SC magnets in the supercritical helium environment. The two cryogenic subsystems for SC facilities have been put into cryogenic operation and beam commissioning since March 2025. Therefore, the performances of two cryogenic subsystems can meet all cooling requirements for the superconducting facilities of BEPCII-U, and successful operation over for the past several months demonstrates that the upgrade design of BEPCII-U cryogenic system is both reasonable and feasible.

Acknowledgments

Supported by BEPC II (Y41G1020Y1).

References

- [1] C. Yu et al., *BEPCII Performance and Beam Dynamics Studies on Luminosity*, in the proceedings of the *7th International Particle Accelerator Conference*, Busan, South Korea, May 8–13 (2016) [[DOI:10.18429/JACoW-IPAC2016-TUYA01](https://doi.org/10.18429/JACoW-IPAC2016-TUYA01)].
- [2] H. Geng et al., *Lattice Design for BEPCII Upgrade*, in the proceedings of the *12th International Particle Accelerator Conference*, Campinas, SP, Brazil, May 24–28 (2021) [[DOI:10.18429/JACoW-IPAC2021-THPAB002](https://doi.org/10.18429/JACoW-IPAC2021-THPAB002)].
- [3] R. Han et al., *Preliminary Design of the BEPCII-Upgrade Cryogenic System*, in the proceedings of the *28th International Cryogenic Engineering Conference and International Cryogenic Materials Conference*, Hangzhou, China, April 25–29 (2022), p. 308–313 [[DOI:10.1007/978-981-99-6128-3_38](https://doi.org/10.1007/978-981-99-6128-3_38)].
- [4] L.X. Jia and L. Wang, *Cryogenic System for BEPCI SRF Cavity IR Quadrupole and Detector Solenoid Magnets*, in the proceedings of the *20th International Cryogenic Engineering Conference*, Beijing, China, May 10–14 (2004), p. 107–110 [[DOI:10.1016/b978-008044559-5/50026-0](https://doi.org/10.1016/b978-008044559-5/50026-0)].
- [5] T.-M. Huang et al., *High power input coupler development for BEPCII 500-MHz superconducting cavity*, *Nucl. Instrum. Meth. A* **623** (2010) 895.
- [6] T. Huang et al., *The development of the 499.8 MHz superconducting cavity system for BEPCII*, *Nucl. Instrum. Meth. A* **1013** (2021) 165649.
- [7] Y. Liu et al., *Cryogenic system for BEPCII superconducting cavities*, in the proceedings of the *13th International Workshop on RF Superconductivity*, Beijing China, October 14–19 (2007), p. 486–488, <https://accelconf.web.cern.ch/srf2007/PAPERS/WEP19.pdf>.
- [8] S. Li et al., *Overall Design of the ADS Injector I Cryogenic System in China*, *Phys. Procedia* **67** (2015) 863.
- [9] H. Zheng et al., *Development and tests of the 499.8 MHz srf cryomodules for HEPS*, *2024 JINST* **19** P10031.
- [10] R. Han et al., *Thermal performance analysis and cryogenic experimental measurements of the 166.6 MHz cavity cryomodule for the High Energy Photon Source*, *Nucl. Instrum. Meth. A* **1070** (2025) 170000.
- [11] HEPAC, Cryodata, Inc.

- [12] Y. Zhu, Y. Wu and W. Kang, *Magnetic Field Simulation of Serpentine Quadrupole Coil*, *IEEE Trans. Appl. Supercond.* **22** (2012) 4901105.
- [13] C.H. Yu et al., *Interaction region design and realization for the Beijing Electron Positron Collider*, *Nucl. Instrum. Meth. A* **608** (2009) 234.
- [14] Y.Z. Wu et al., *The Magnet System of the BEPCII Interaction Region*, *IEEE Trans. Appl. Supercond.* **20** (2010) 360.
- [15] J. Geng et al., *Direct wind control software of the BEPCII Upgrade superconducting magnet*, *Radiat. Detect. Technol. Methods* **9** (2025) 545.
- [16] P. Li et al., *The design and testing of the gas-cooled high-temperature superconducting current leads for BEPCII-Upgrade*, *Nucl. Instrum. Meth. A* **1082** (2026) 171052.
- [17] N.A. Mezentsev and E.A. Perevedentsev, *Survey of Superconducting Insertion Devices for Light Sources*, in the proceedings of the *Particle Accelerator Conference*, Knoxville, TN, U.S.A., May 16–20 (2005) [DOI:10.1109/pac.2005.1590409].
- [18] A.A. Volkov et al., *Superconducting 119-pole wiggler with a 2.1-T field and 30-mm period length for the ALBA storage ring*, *J. Surf. Invest.* **6** (2012) 379.
- [19] D. Schoerling et al., *Design and system integration of the superconducting wiggler magnets for the Compact Linear Collider damping rings*, *Phys. Rev. ST Accel. Beams* **15** (2012) 042401.
- [20] M. Xu et al., *Design and Research of Cryostat for 3WI Superconducting Wiggler Magnet*, *IEEE Trans. Appl. Superconduct.* **28** (2018) 1.
- [21] T. Nakamoto et al., *Construction of Superconducting Magnet System for the J-PARC Neutrino Beam Line*, *IEEE Trans. Appl. Supercond.* **20** (2010) 208.
- [22] B. Parker et al., *Compact Superconducting Final Focus Magnet Options for the ILC*, in the proceedings of the *Particle Accelerator Conference*, Knoxville, TN, U.S.A., May 16–20 (2005), p. 1569–1571 [DOI:10.1109/pac.2005.1590838].
- [23] BNL Magnet Division, *Design report for the BEPCII superconducting IR magnets*, AM-NO 328, Brookhaven National Laboratory, Upton, NY, U.S.A. (2003).